ADVANCES IN ATMOSPHERIC SCIENCES, VOL. 29, NO. 3, 2012, 509–518

Variations of the Summer Somali and Australia Cross-Equatorial Flows and the Implications for the Asian Summer Monsoon

ZHU Yali*[1,2] (祝亚丽)

[1] *Nansen-Zhu International Research Centre, Institute of Atmospheric Physics, Chinese Academy of Sciences, Beijing* 100029

[2] *Climate Change Research Center, Chinese Academy of Sciences, Beijing* 100029

(Received 14 July 2011; revised 23 November 2011)

ABSTRACT

The temporal variations during 1948–2010 and vertical structures of the summer Somali and Australia cross-equatorial flows (CEFs) and the implications for the Asian summer monsoon were explored in this study. The strongest southerly and northerly CEFs exist at 925 hPa and 150 hPa level, respectively. The low-level Somali (LLS) CEFs were significantly connected with the rainfall in most regions of India (especially the monsoon regions), except in a small area in southwest India. In comparison to the climatology, the low-level Australia (LLA) CEFs exhibited stronger variations at interannual time scale and are more closely connected to the East Asian summer monsoon circulation than to the LLS CEFs.

The East Asian summer monsoon circulation anomalies related to stronger LLA CEFs were associated with less water vapor content and less rainfall in the region between the middle Yellow River and Yangtze River and with more water vapor and more rainfall in southern China. The sea-surface temperature anomalies east of Australia related to summer LLA CEFs emerge in spring and persist into summer, with implications for the seasonal prediction of summer rainfall in East Asia. The connection between the LLA CEFs and East Asian summer monsoon rainfall may be partly due to its linkage with El Nino-Southern Oscillation. In addition, both the LLA and LLS CEFs exhibited interdecadal shifts in the late 1970s and the late 1990s, consistent with the phase shifts of Pacific Decadal Oscillation (PDO).

Key words: cross-equatorial flow, Asian summer monsoon, low-level jet, Somali

Citation: Zhu, Y. L., 2012: Variations of the summer Somali and Australia cross-equatorial flows and the implications for the Asian summer monsoon. *Adv. Atmos. Sci.*, **29**(3), 509–518, doi: 10.1007/s00376-011-1120-6.

1. Introduction

Cross-equatorial flows (CEFs) in the lower levels of the atmosphere are important conveyers of water vapor between the winter and summer hemispheres, and they have attracted much attention from meteorologists. CEFs have significant implications for climate in many regions not only for climatology but also at the synoptic scale (Xu, 2011). Located over the equatorial oceans in boreal summer (June–July–August) and strongest at 925 hPa, CEFs mainly transport water vapor from the Southern to the Northern Hemisphere in the following regions: the east coast of Somali, north of Australia, the eastern Pacific and Atlantic oceans (Fig. 1) (e.g., Wang and Xue, 2003). Among them, the Somali CEF is the strongest and has been the focus of much study since Findlater discovered it in the 1960s (i.e., Findlater, 1969). The Somali CEFs are located over the Somali coast near the East African Mountains, turn southwesterlies in the Arabian Sea and together with the southwesterlies over the Arabian Sea are often called the Somali low-level jet.

The formation of the Somali low-level jet can be attributed to several factors, including the East African Mountains, the beta effect, land–sea contrast, baroclinicity in the boundary layer, diabetic heating, with diverse emphasis on the dominating factors in different studies (Krishnamurti et al., 1976; Krishnamurti and Wong, 1979; Rodwell and Hoskins, 1995). Using a general circulation model (GCM), Chakraborty et al.,

*Corresponding author: ZHU Yali, zhuyl@mail.iap.ac.cn

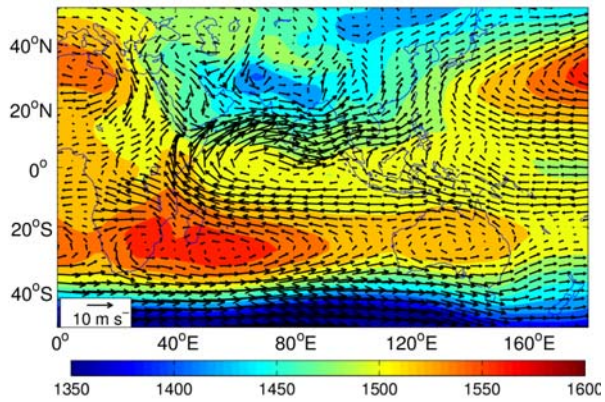

Fig. 1. Climatology of wind (arrows, units: m s^{-1}) and geopotential height (shadings, units: gpm) at 850 hPa in summer during 1980–1999.

(2009) determined that the CEFs occur even in the absence of the African orography, which only intensifies the CEFs; the longitudinal location of the Somali CEFs depends upon the diabetic heating of the Indian monsoon, while the vertical structure depends on the western boundary current in the atmosphere due to the East African highlands. Using atmospheric GCM (AGCM) simulations with different mountains, Xu et al. (2010) also found that the presence of African-Arabian mountains can strengthen the CEFs in the lower and upper levels over East Africa.

In terms of climate, the Somali CEFs provide most of the water vapor for the Asian summer monsoon. In summer, water vapor originates from the southern Indian Ocean, flows into the Arabian Sea via the Somali jet, then largely passes the India Peninsula, the Bay of Bengal, the Indo-China Peninsula, and then partly arrives in East Asia (Fig. 1).

CEFs are regarded as an important member of the South and East Asian summer monsoon systems (Ding, 2005); they have been widely studied by meteorologists (e.g., Dube et al., 1990; Halpern and Woiceshyn, 1999, 2001; Kulkarni et al., 2002; Wang and Xue, 2003; Joseph and Sijikumar, 2004). Australia CEFs are another important water vapor source for the East Asian summer monsoon. They originate from the South Pacific, branch from the anticyclone related to the Australian high (AH), and cross the equator in the western Pacific. Some studies have shown the Australia CEFs to be connected with Asian summer rainfall (Wang and Li, 1982; Li et al., 2004; Lei and Yang, 2008).

Usually, previous studies have been based on original data. However, original data includes variations at multiple time scales, such as interannual and interdecadal time scales. Variations at different time scales are often related to distinct physical and dynamical processes. It is possible that a positive correlation exists between two systems at interannual time scale, while a negative correlation exists at interdecadal or longer time scale. Thus the correlation of the original data may be weakened or may not be revealed. To separate the signals at interannual and interdecadal (or longer) time scales, a Butterworth filter with the window width of nine cases (9-year Butterworth filter) was used in the current study.

In this study, we focused on the temporal features and vertical structure of both the Somali and Australia CEFs, and we compared their relative roles in the connection with the Asian summer monsoon. The NCEP/NCAR reanalysis dataset (Kalnay et al., 1996), 160-station rainfall observation data of China (downloaded from the website of China National Climate Center), and the subregion rainfall data of India (downloaded from the website of Indian Institute of Tropical Meteorology) were used in this study. Because the satellite data were incorporated into the reanalysis after the late 1970s (Sterl, 2004), which increases the reliability of the reanalysis, we focused on the period 1979–2010.

2. Temporal variations and vertical structure

The areal mean (10°N–10°S, 35°–65°E) meridional wind data in summer at different levels was used to investigate the temporal evolution and vertical structure of the Somali CEFs (Fig. 2). Corresponding to the low-level southerlies, Somali CEFs are strongest at 925 hPa, while relatively weaker northerlies exist in the upper level, with a maximum at 150 hPa. The upper-level Somali CEFs became obviously weaker after the 1960s, and especially after the 1990s (Figs. 2a and b). The low-level (925-hPa) Somali (LLS) CEFs became stronger after the late 1970s and weaker after the late 1990s. The two transitions are likely related to the interdecadal changes in the summer rainfall pattern in East China during the late 1970s (Wang, 2001, 2002; Krishnan and Sugi, 2003; Kang and Wang, 2005; Jiang and Wang, 2005; Zhou et al., 2006; Han and Wang, 2007; Zhao et al., 2010; Wu et al., 2010) and the late 1990s (Sun et al., 2011; Zhu et al., 2011), respectively. The decadal cooling and decreased rainfall in the Indian summer monsoon after late 1990s (Yun et al., 2010) may be also closely connected to the weakening of the Somali CEFs. At $\sim$ 850 hPa, the Somali CEFs show a strong upward trend, with two marked increases in strength in the late 1970s and the late 1990s.

The low-level Australia (LLA) CEFs (10°N–10°S, 100°–140°E) were much weaker than the LLS CEFs,

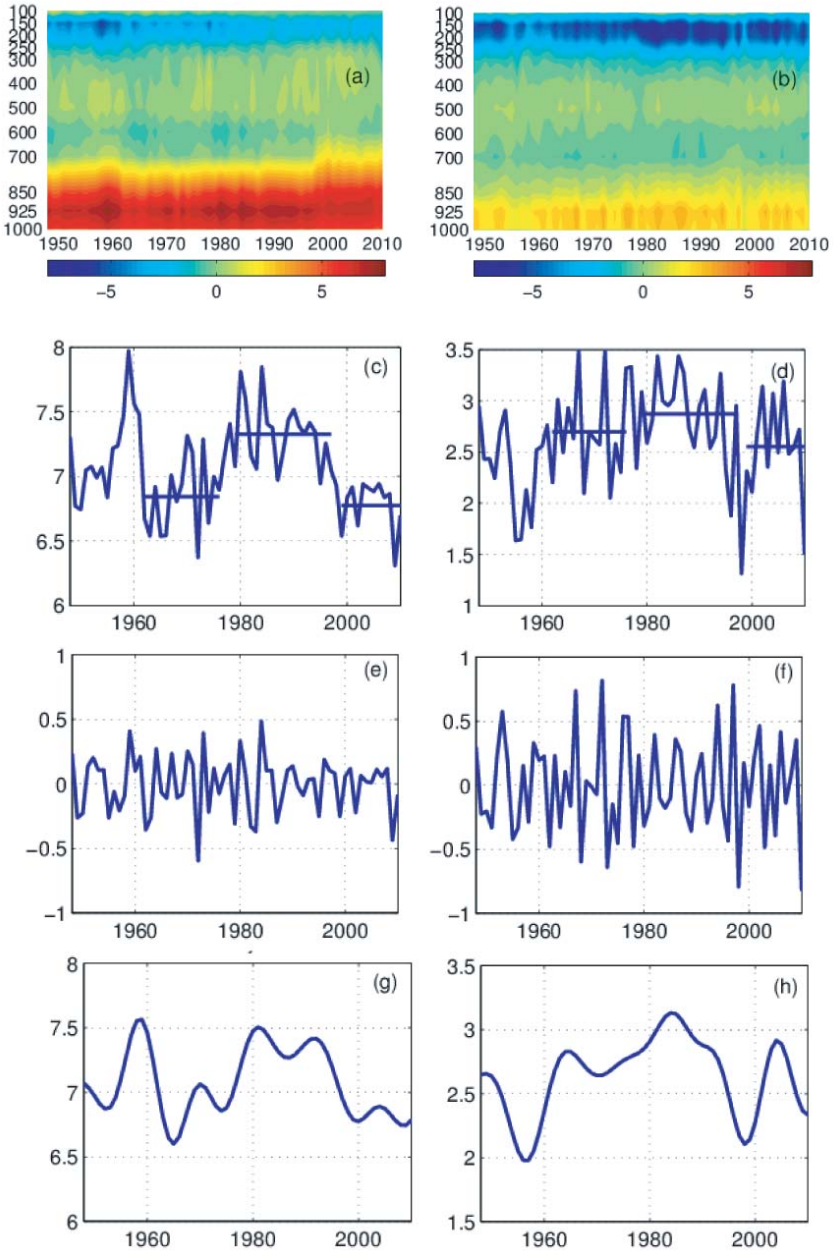

Fig. 2. Areal mean meridional wind over (a) the Somali CEF regions, (b) the Australia CEF regions; (c) original LLS CEFs, and (d) LLA CEFs; (e) 9-year high-pass filtered LLS CEFs, and (f) LLA CEFs; (g) 9-year low-pass filtered LLS CEFs, and (h) LLA CEFs. Units: m s^{-1}.

but with almost synchronous decadal time scale shifts in the late 1970s and the late 1990s (Figs. 2c, d, g, h). However, the upper-level Australia CEFs were much stronger than the Somali branch, and they became stronger after the 1980s. Though the LLS CEFs were much stronger than the LLA CEFs, the standard deviation (SD) of the latter was much higher for the original CEFs (LLA CEF SD = 0.59, LLS CEF SD = 0.35), and the SDs were 0.45 and 0.22 for the LLA CEF and the LLS CEF, respectively, for the interannual time scale (retrieved via 9-year high-pass Butterworth filter; Figs. 2c–f).

3. Implications for the Asian summer rainfall

3.1 *South Asian summer rainfall*

Parthasarathy et al. (1995) investigated the Indian rainfall in homogeneous regions and meteo-

rological subdivisions that were also used in this study. (The divisions of homogeneous regions are not shown here and can be found at the website: http://www.tropmet.res.in/IITM/region-maps.html.) Table 1 lists the correlation coefficients between the LLS CEFs and the LLA CEFs, respectively, and the areal mean rainfall in these regions.

Significant positive correlations were found between the LLS CEFs at the interannual and interdecadal (and longer) time scales and rainfall in five regions: all-India, homogeneous monsoon regions, core monsoon regions, west central India, central northeast India. Rainfall in the northeast, northwest, and peninsular regions of India were not significantly related to LLS CEFs. The relationships between regional rainfall and LLS CEFs were consistent with those between the water vapor fluxes and the LLS CEFs. When the LLS CEFs were stronger, the southwesterlies transporting water vapor into India were strengthened, and water vapor content in most regions of India increased (except in small parts of northeastern, northwestern, and southwestern India), and thus more rainfall occurred in these regions. An interesting phenomenon is the significant correlation between LLA CEFs and the rainfall in the Indian Peninsula. When the LLA CEFs were stronger, less water vapor was transported into southern tip of India (Fig. 4a), and less rainfall occurred there.

3.2 *East Asian summer rainfall*

Traditionally, the LLS CEFs have been thought to be more important than the LLA CEFs because they can bring one to two times more water vapor to the East Asian summer monsoon. Thus, we computed the correlation between the LLS/LLA CEFs and observation rainfall data in China during 1979–2010 (Fig. 3). Our comparison shows that the LLA CEFs have a stronger connection with rainfall than do the LLS CEFs for both the original data and the interannual time scale variation (9-year high-pass filtered; Figs. 3a–d). Only a few scattered significant correlations were found for LLS CEFs, while for LLA CEFs, significant values appeared between the middle Yellow River and Yangtze River, which became even stronger on the interannual time scale (Figs. 3c and d). Thus, it is reasonable to conclude that the LLS CEFs can bring more water vapor to the East Asian climate in summer but that the LLA CEFs are more closely connected with the monsoon rainfall at an interannual time scale. For the interdecadal and longer time scales (9-year low-pass filtered), LLA CEFs and LLS CEFs showed a correlation pattern similar to that of rainfall observations, that is, a positive correlation north of the Yangtze River and a negative correlation south of the Yangtze River. Two regional mean rainfall indices were defined for the area between the middle Yellow River and the Yangtze River (30°–35°N, 100°–110°E, P1) and southern China (23°–26°N, 100°–120°E, P2). Their correlations with the LLS CEFs were insignificant at the interannual time scale (Table 2). The LLA CEFs were significantly correlated with P1 (-0.74) and P2 (0.65) at the interannual time scale (Figs. 3g and h). The correlations at interdecadal and longer time scales were also significant, but with opposite signs to the interannual data (0.55 for P1 and -0.77 for P2), which resulted in the weaker correlations between the original LLA CEFs and P1 (correlation coefficient $= -0.4$) and P2 (correlation coefficient $= 0.02$).

When the LLA CEFs were stronger, large-scale flux anomalies appeared over the tropical Pacific and Indo-Pacific Ocean, with westerly and easterly anomalies in the southwestern and northeastern parts, respectively. Accordingly, in the correlation regarding water vapor content, two northwest–southeast belts were seen, with more water vapor in the southwestern part and less in the northeastern part (Fig. 4b). Stronger LLA CEFs were related to less water vapor content over most part of Australia, the maritime continent to the north, and part of the South Pacific Ocean to the east, while they were related to more water vapor over most part of the tropical Pacific. In accordance with the anomalies shown in rainfall observation data (Fig. 3), there was less water vapor (i.e., decreased rainfall) in the area between the middle Yellow River and Yangtze River, and more water vapor (i.e., increased rainfall) in southern China. In addition, stronger LLA CEFs were associated with easterly anomalies in the eastern tropical Pacific ($\sim 0°$–20°N), weaker LLS CEFs, and stronger Australian high. Thus, the LLA and LLS CEFs are not fully independent of each other; they are all partly linked with the Southern Hemispheric circulation, particularly the Mascarene High and the Australian high (Xue et al., 2003).

In general, the area affected by LLS CEFs was smaller than that affected by LLA CEFs (Fig. 4a). Stronger LLS CEFs were related to southwesterly wind anomalies over the Arabian Sea, which can bring more water vapor to the Indian summer monsoon region (Chakraborty et al., 2009) and thus more rainfall over most regions in India (Table 1) Anomalous signals also appeared over the Pacific Ocean: easterly anomalies were seen over the central-eastern tropical Pacific, and cyclonic and anticyclonic anomalies were seen over the North Pacific. Though the LLS CEFs originated from the Southern Hemisphere, subtle signals appeared over the Southern Ocean, with the exception of significant cyclonic wind anomalies southeast of the Australian

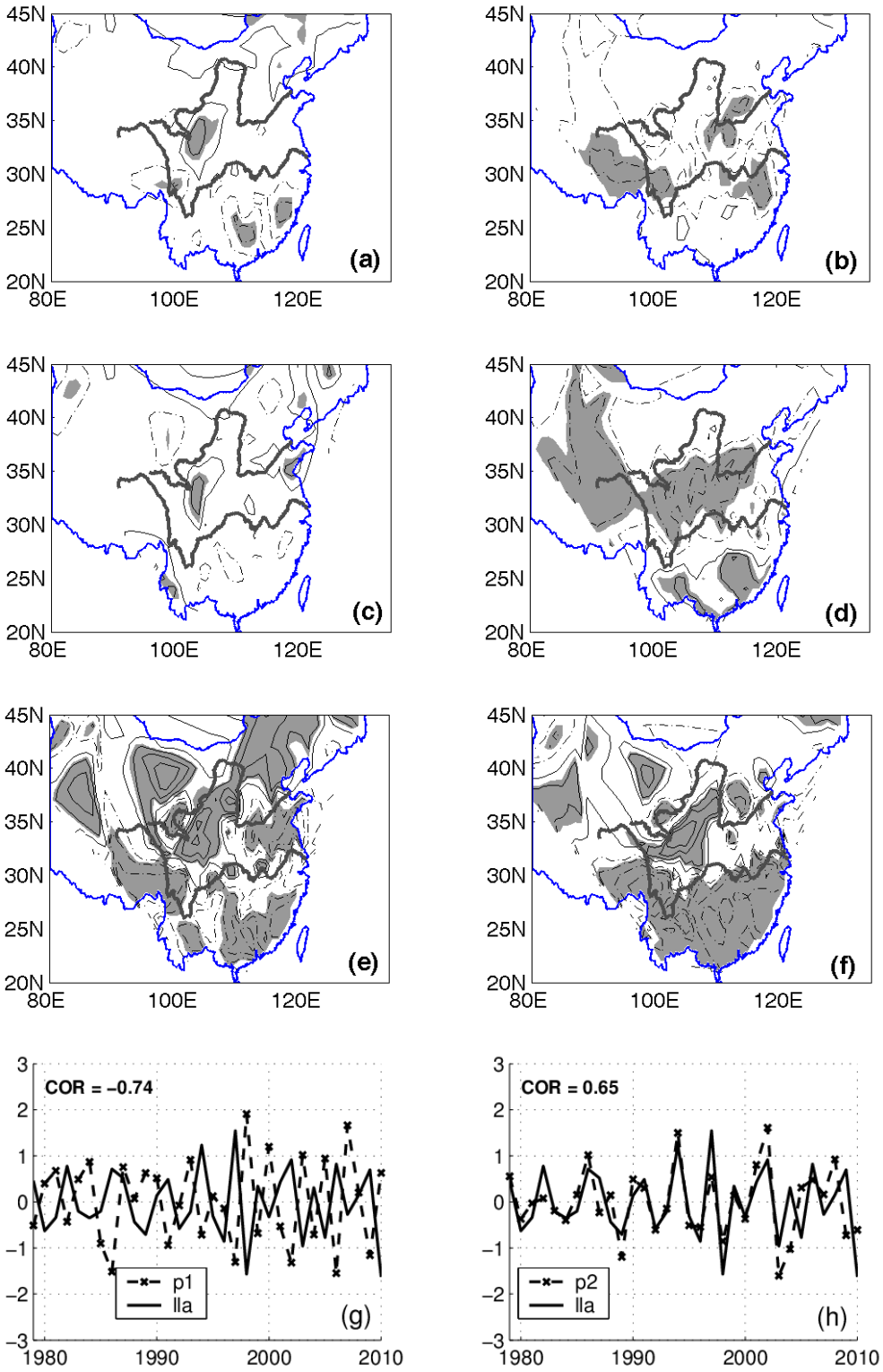

Fig. 3. Correlations between (a, b) the original data, (c, d) 9-year high-pass filtered data; (e, f) 9-year low-pass filtered data. LLS CEFs and LLA CEFs and 160-station summer rainfall observation data during the period 1979–2010. Shadings represent significant values at the 95% confidence level. Contour values are −0.6, −0.4, −0.2, 0.2, 0.4, 0.6. The two thick curves show the location of the Yellow River and the Yangtze River. (g, h) The 9-year high-pass filtered regional mean rainfall indices and LLA CEFs during 1979–2010.

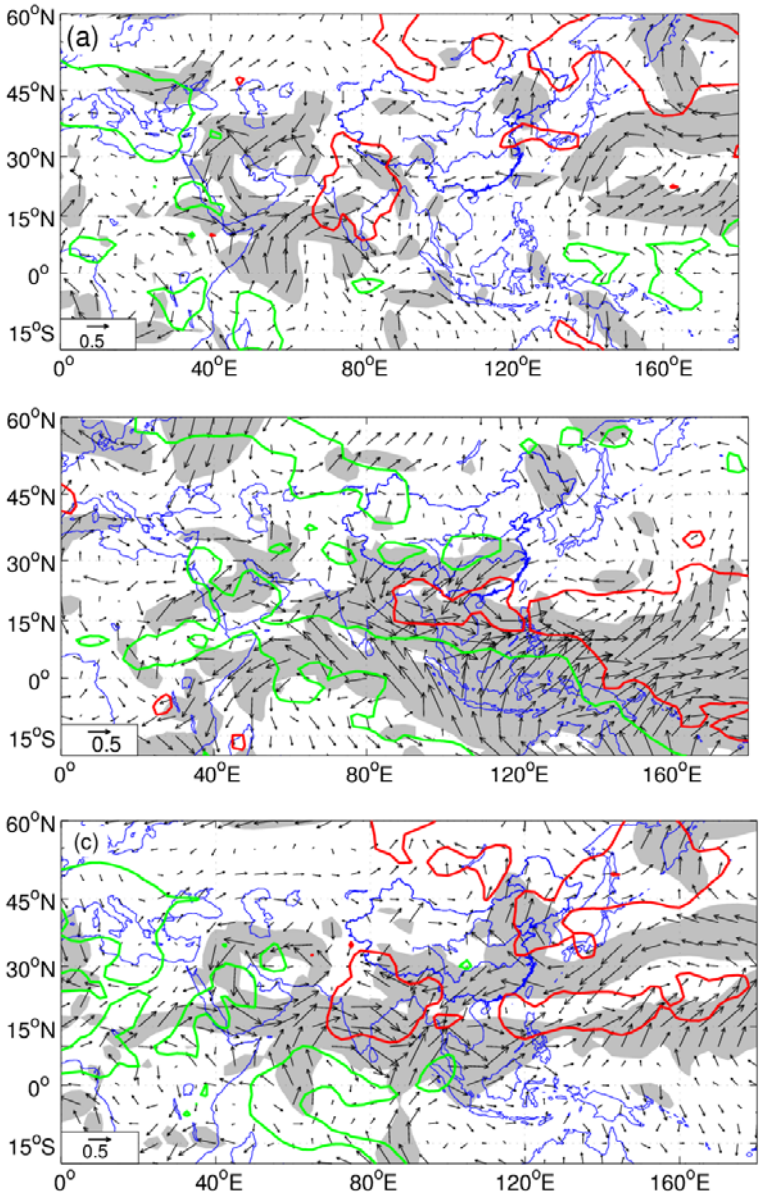

Fig. 4. Correlations between (a) the LLS CEFs, (b) LLA CEFs, (c) Somali low-level jet and the vertically integrated (300–1000 hPa) water vapor flux (arrows) and water vapor content for the 9-year high-pass filtered data. Contours represent significant correlations at 95% confidence level: red/green for positive/negative values. Shadings represent significant correlations for the wind field at 95% confidence level.

high.

4. Connections with SST

In the correlation with global SST (Fig. 5), the LLS CEFs were negatively associated with the SST in the western tropical Indian Ocean, the Arabian Sea, and the central-eastern tropical Pacific. The LLA CEFs were significantly negatively correlated with the local SST (Indo-Pacific and the subtropical Pacific to the east of Australia) and were positively linked with the SST in the central-eastern Pacific, showing its significant connection with El Niño/Southern Oscillation (ENSO). Previous studies have also revealed that ENSO events are closely associated with the LLS and LLA CEFs at an interannual time scale. Chen et al. (2005) showed that in El Niño years, LLS CEFs become weaker, while LLA CEFs become stronger.

Table 1. The correlation coefficients between LLS/LLA CEFs and regional rainfall in India for the period 1979–2010. Bold numbers indicate significant correlations at 95% confidence level using a Student's t-test.

	Original		Interannual		Interdecadal	
Regions	LLS	LLA	LLS	LLA	LLS	LLA
All-India	**0.45**	−0.11	**0.61**	−0.16	**0.39**	−0.07
Homogeneous monsoon region	**0.42**	−0.04	**0.44**	−0.13	**0.54**	0.19
Core monsoon region	**0.45**	0.14	**0.46**	0.02	**0.55**	**0.39**
Northwest India	0.24	−0.2	**0.35**	−0.21	0.14	−0.20
West central India	**0.45**	0.08	**0.43**	−0.06	**0.78**	**0.55**
Central northeast India	**0.33**	0.02	**0.69**	0.1	**−0.45**	**−0.45**
Northeast India	0.04	−0.09	−0.02	−0.12	0.1	−0.21
Indian Peninsula	0.21	**−0.44**	0.2	**−0.55**	**0.34**	−0.19

Note: LLS is low-level Somali cross-equatorial flow; LLA is low-level Australia cross-equatorial flow.

Table 2. The correlation coefficient between LLS/LLA CEFs and regional mean summer rainfall in China for the period 1979–2010. Bold numbers indicate significant correlations at 95% confidence level using a Student's t-test.

	Original (9-year high-pass)		Interannual (9-year low-pass)		Interdecadal (9-year low-pass)	
	P1	P2	P1	P2	P1	P2
LLS CEF	0.24	**−0.35**	0.22	−0.02	**0.45**	**−0.64**
LLA CEF	**−0.4**	0.02	**−0.74**	**0.66**	**0.55**	**−0.77**

Note: LLS is low-level Somali cross-equatorial flow; LLA is low-level Australia cross-equatorial flow.

Significant autocorrelation exists between the LLA CEFs in the spring and following summer at an interannual time scale, with a correlation coefficient of 0.4 during 1979–2010. This seasonal persistence can be attributed to sustained sea surface temperature (SST) anomalies from spring to summer. SST anomalies associated with summer LLA CEFs emerged to the north and east of Australia in spring (Fig. 5) and then spread northward and intensified in summer, accompanying the seasonal advancement of the intertropical convergence zone (Sun et al., 2009). The spring LLA CEFs and summer rainfall observations show a correlation pattern quite similar to that of summer CEFs and rainfall (with negative values in the region between middle Yellow River and Yangtze River and positive in southern China), though the significant area was much smaller (not shown). Thus, the LLA CEFs and related SST anomalies in spring can provide some information for the East Asian summer rainfall prediction. However, for the LLS CEFs, such seasonal persistence did not exist. To show the connection of LLS and LLA CEFs with SST more clearly, the regional mean SSTs in summer were calculated over the Arabian Sea (10°S–10°N, 50°–70°E, SST_{Arab}) and east of Australia (20°–35°S, 160°–180°E, SST_{Austr}), respectively. The LLS CEFs, LLA CEFs, SST indices, and Southern Oscillation index (SOI) from 1979 to 2010 were plotted in Fig. 5d. The correlation coefficients between LLS CEFs and SST_{Arab} were -0.63 for the original time series and −0.58 for the interannual time scale. The correlation coefficients between LLA CEFs and summer SST_{Austr} were −0.71 for the original time series and −0.76 for the interannual time scale. The correlation coefficient between LLA CEFs and spring SST_{Austr} were −0.52 for the original time series and −0.48 for the interannual time scale. In addition, the SOI and SST_{Austr} were not independent but had a correlation coefficient of 0.59. As the second mode of the southern high-latitude geopotential height field (Karoly, 1989), the Pacific–South America teleconnection pattern is a major atmospheric response to ENSO in the Southern Hemisphere, and it was also significantly associated with the LLA CEFs (correlation coefficient is −0.37).

5. Brief discussion and summary

The temporal features and vertical structure of the Somali and Australia CEFs were investigated in this study. In boreal summer, strong southerly CEFs exist over the Somali region and north of Australia at low atmospheric levels; they are strongest at the 925 hPa. Upper-level northerly CEFs north of Australia are much stronger than the Somali CEFs. The im-

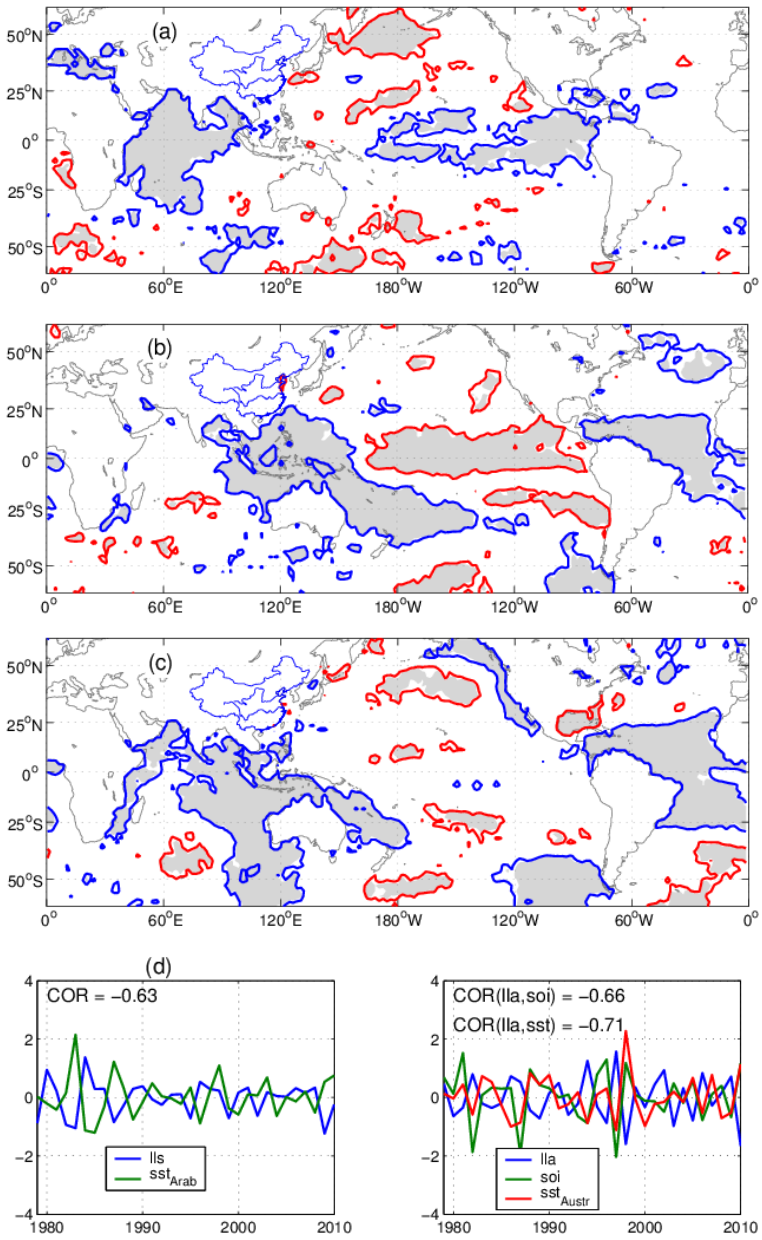

Fig. 5. Using 9-year high-pass filtered data, correlations between (a) summer LLS CEFs and summer SST; (b) summer LLA CEFs and summer SST; and (c) summer LLA CEFs and SST in the preceding spring. Shading indicates significant values at the 95% confidence level. The red contour is 0.3 and the blue contour is −0.3. (d) LLS and LLA CEFs, regional mean SST indices, and SOI during 1979–2010.

plications of the LLS CEFs and LLA CEFs for the Asian summer monsoon rainfall and their relative roles were also explored. Stronger LLS CEFs are connected with stronger southwesterly winds in the Arabian Sea, which can bring more water vapor and thus more rainfall into the Indian monsoon region, but LLS CEFs have a very weak correlation with the low-level wind and water vapor content over East Asia. The stronger correlation between the LLA and East Asian summer rainfall and the weaker correlation between the LLS and East Asian summer rainfall are consistent with the finding that convective activities over the Asian monsoon region are more closely associated with the convective activities over the western subtropical Pacific (connected with the LLA) than with those over the northern tropical Indian Ocean (connected with

the LLS; Li et al., 2010). The weak connection between the LLS CEFs and East Asian summer monsoon circulation is understandable: the LLS CEFs pass over the Arabian Sea, the Indian monsoon region, the Bay of Bengal, and the Indo-China Peninsula before they finally arrive in East Asia, and variable factors during this process may influence the final conditions of the water vapor which originate from the LLS CEFs. Thus the connection with rainfall in East Asia at an interannual time scale is subtle and difficult to detect.

Though climatically the LLA CEFs are much weaker than the LLS CEFs, they exhibited stronger interannual variation, with an SD of 0.59 for the original LLA CEFs and an SD of 0.35 for the original LLS CEFs, and an SD of 0.45 for LLA CEFs on an interannual time scale and an SD of 0.22 for the LLS CEFs for the interannual time scale (9-year high-pass filtered). Stronger LLA CEFs were significantly related with less water vapor content and less rainfall over the region between the middle of the Yellow River and Yangtze River, as well as the southern tip of the Indian Peninsula. Both CEFs were significantly correlated with SST in the central-eastern tropical Pacific, but with opposite signs. The LLA CEFs were significantly related to the local SST anomalies to the north and east of Australia. The local SST anomalies (north and east of Australia) emerge in spring, persist, and advance northward with the seasonal cycle in summer (Sun et al., 2009); thus the LLA CEFs and the local SST anomalies in spring can provide some information about the summer rainfall in East Asia, especially over southern China and the region between the middle Yellow River and Yangtze River. The SST east of Australia is also significantly related with the ENSO phenomenon at an interannual time scale, which manifests the entangled connections in the climate system. The important role of the SST east of Australia has been also revealed by Zhou and Cui (2011): positive SST anomalies east of Australia in spring are followed by a cyclonic circulation anomaly in the upper troposphere and an anticyclonic circulation anomaly in the lower troposphere over the western North Pacific from June to October, concurrent with anomalous atmospheric subsidence and an enlarged vertical zonal wind shear, which are unfavorable for tropical cyclone genesis.

The LLS CEFs are significantly related with the southwesterly low-level jet in the Arabian Sea (5°–20°N, 60°–80°E, Fig. 4c). Stronger low-level jet corresponds to more water vapor content over Indian summer monsoon region, cyclonic wind anomalies in the northwestern Pacific, with easterly anomalies over southern China, and southerly anomalies and increased water vapor content over Northeast and eastern part of North China. Thus, the low-level jet in the Arabian Sea is more closely associated with the East Asian monsoon circulation compared to the LLS CEFs.

In addition, at interdecadal timescale (9-year low-pass filtered), the correlation pattern between the LLA CEFs and global SST is quite similar with that of LLS CEFs, showing a PDO-like pattern over the Pacific, with positive/negative correlation in the eastern tropical Pacific/North and South Pacific (not shown). This result provides more evidence for the important role of PDO in the climate system at interdecadal scale (e.g., Mantua and Hare, 2002; Zhu et al., 2011).

Acknowledgements. This study was jointly supported by the National Basic Research Program of China (Grant Nos. 2009CB421406 and 2010CB950304), the Special Fund for the Public Welfare Industry (Meteorology; Grant Nos. GYHY201006022 and GYHY200906018), and the strategic technological program of the Chinese Academy of Sciences (Grant No. XDA05090405).

REFERENCES

Chakraborty, A., R. S. Nanjundiah, and J. Srinivasan, 2009: Impact of African orography and the Indian summer monsoon on the low-level Somali jet. *Int. J. Climatol.*, **29**, 983–992.

Chen, B., P. W. Guo, and Y. C. Xiang, 2005: Relationship between summer cross-equatorial flows and ENSO. *Journal of Nanjing Institute of Meteorology*, **28**, 36–43. (in Chinese)

Ding, Y. H., 2005: *Advanced Synoptic Meteorology*. China Meteorological Press, 585pp. (in Chinese)

Dube, S. K., M. E. Luther, and J. J. O'Brien, 1990: Relationships between interannual variability in the Arabian Sea and Indian summer monsoon rainfall. *Meteor. Atmos. Phys.*, **44**, 153–165.

Findlater, J., 1969: A major low-level air current near Indian Ocean during Northern Summer. *Quart. J. Roy. Meteor. Soc.*, **95**, 362–380.

Halpern, D., and P. M. Woiceshyn, 1999: Onset of the Somali Jet in the Arabian Sea during June 1997. *J. Geophys. Res.*, **104**, 18041–18046.

Halpern, D., and P. M. Woiceshyn, 2001: Somali Jet in the Arabian Sea, El Niño, and India rainfall. *J. Climate*, **14**, 434-441.

Han, J. P., and H. J. Wang, 2007: Interdecadal variability of the East Asian summer monsoon in an AGCM. *Adv. Atmos. Sci.*, **24**, 808–818, doi: 10.1007/s00376-007-0808-0.

Jiang, D. B., and H. J. Wang, 2005: Natural interdecadal weakening of East Asian summer monsoon in the late 20th century. *Chinese Sci. Bull.*, **50**, 1923–1929.

Joseph, P. V., and S. Sijikumar, 2004: Intraseasonal variability of the low-level jet stream of the Asian summer monsoon. *J. Climate*, **17**, 1449–1458.

Kalnay, E., and Coauthors, 1996: The NCEP/NCAR 40-Year Reanalysis Project. *Bull. Amer. Meteor. Soc.*, **77,** 437–471.

Kang, D. J., and H. J. Wang, 2005: Analysis on the decadal scale variation of the dust storm in North China. *Science in China* (*D*), **48**, 2260–2266.

Karoly, D. J., 1989: Southern Hemisphere circulation features associated with El Niño-Southern Oscillation events. *J. Climate*, **2**, 1239–1251.

Krishnamurti, T. N., and V. Wong, 1979: Planetary Boundary-Layer Model for the Somali Jet. *J. Atmos. Sci.*, **36**, 1895–1907.

Krishnamurti, T. N., J. Molinari, and H. L. Pan, 1976: Numerical-simulation of Somali Jet. *J. Atmos. Sci.*, **33,** 2350–2362.

Krishnan, R., and M. Sugi, 2003: Pacific decadal oscillation and variability of the Indian summer monsoon rainfall. *Climate Dyn.*, **21**, 233–242, doi: 10.1007/s00382-003-0330-8.

Kulkarni, J. R., Vinaykumar, and V. Satyan, 2002: The association of surface wind stresses over Indian Ocean with monsoon rainfall. *Meteorol. Atmos. Phys.*, **79**, 231–242.

Lei, X. C., and X. Q. Yang, 2008: interannual variation characteristics of East Hemispheric cross-equatorial flow and its contemporaneous relationships with temperature and rainfall in China. *Journal of Tropical Meteorology*, **24**, 127–135. (in Chinese)

Li, X. H., H. M. Xu, and J. H. He, 2004: the study on the relationship between the west cross-equatorial flow and the heavy rain in South China. *Scientia Meteorologica Sinica*, **24**, 161–167. (in Chinese)

Li, Y. F., Z. N. Xiao, J. H. Ju, and G. Q. Hu, 2010: The variations of dominant convection modes over Asia, Indian Ocean, and western Pacific Ocean during the summers of 1997–2004. *Adv. Atmos. Sci.*, **27**, 901–920, doi: 10.1007/s00376-009-9072-9.

Mantua, N. J., and S. R. Hare, 2002: The Pacific decadal oscillation.. *J. Oceanogr.*, **58**, 35–44.

Parthasarathy, B., A. A. Munot, and D. R. Kothawale, 1995: Monthly and seasonal rainfall series for all-India homogeneous regions and meteorological subdivisions: 1871–1994. Research Report No. RR-065, Indian Institute of Tropical Meteorology, 113pp.

Rodwell, M. J., and B. J. Hoskins, 1995: A model of the Asian summer monsoon. 2. Cross-equatorial flow and Pv behavior. *J. Atmos. Sci.*, **52**, 1341–1356.

Sterl, A., 2004: On the (In)homogeneity of reanalysis products. *J. Climate*, **17**, 3866–3873.

Sun, B., Y. L. Zhu, and H. J. Wang, 2011: The recent interdecadal and interannual variation of water vapor transport over eastern China. *Adv. Atmos. Sci.*, **28**(5), 1039–1048, doi: 10.1007/s00376-010-0093-1.

Sun, J. Q., H. J. Wang, and W. Yuan, 2009: A possible mechanism for the co-variability of the boreal spring Antarctic Oscillation and the Yangtze River valley summer rainfall. *Int. J. Climatol.*, **29**, 1276–1284, doi: 10.1002/joc.1773.

Wang, H. J., 2001: The weakening of Asian monsoon circulation after the end of 1970s. *Adv. Atmos. Sci.*, **18**, 376–386.

Wang, H. J., 2002: The instability of the East Asian summer monsoon—ENSO relations. *Adv. Atmos. Sci.*, **19**, 1–11.

Wang, H. J., and F. Xue, 2003: Interannual variability of Somali Jet and its influences on the inter-hemispheric water vapor transport and on the East Asian summer rainfall. *Chinese J. Geophys.*, **46**, 18–25. (in Chinese)

Wang, J. Z., and M. C. Li, 1982: Cross-equator flow from Australia and monsoon over China. *Chinese J. Atmos. Sci.*, **6**, 1–10. (in Chinese)

Wu, R. G., Z. P. Wen, S. Yang, and Y. Q. Li, 2010: An interdecadal change in southern China summer rainfall around 1992/93. *J. Climate*, **23**, 2389–2403.

Xu, Y. M., 2011: The genesis of tropical cyclone Bilis (2000) associated with cross-equatorial surges. *Adv. Atmos. Sci.*, **28**, 665–681, doi: 10.1007/s00376-010-9142-z.

Xu, Z. F., Y. F. Qian, and C. B. Fu, 2010: The role of land-sea distribution and orography in the Asian monsoon. Part II: Orography. *Adv. Atmos. Sci.*, **27**, 528–542, doi: 10.1007/s00376-009-9045-z.

Xue, F., H. J. Wang, and J. H. He, 2003: Interannual variability of Mascarene high and Australian high and their influences on summer rainfall over East Asia. *Chin. Sci. Bull.*, **48**, 492–497.

Yun, K. S., K. J. Ha, B. Wang, and R. Q. Ding, 2010: Decadal cooling in the Indian summer monsoon after 1997/1998 El Niño and its impact on the East Asian summer monsoon. *Geophys. Res. Lett.*, **37**, doi: 10.1029/2009GL041539.

Zhao, P., S. Yang, and R. C. Yu, 2010: Long-term changes in rainfall over Eastern China and large-scale atmospheric circulation associated with recent global warming. *J. Climate*, **23**, 1544–1562.

Zhou, B. T., and X. Cui, 2011: Sea surface temperature east of Australia: A predictor of tropical cyclone frequency over the western North Pacific? *Chinese Sci. Bull.*, **56**, 196–201, doi: 10.1007/s11434-010-4157-5.

Zhou, W., C. Y. Li, and J. C. L. Chan, 2006: The interdecadal variations of the summer monsoon rainfall over South China. *Meteorol. Atmos. Phys.*, **93**(3–4), 165–175, doi: 10.1007/S00703-006-018-9.

Zhu, Y. L., H. J. Wang, W. Zhou, and J. H. Ma, 2011: Recent changes in the summer precipitation pattern in East China and the background circulation. *Climate Dyn.*, **36**, 1463–1473, doi: 10.1007/s00382-010-0852-9.